AD

TECHNICAL REPORT ARBRL-TR-02081

OSCILLATIONS OF A LIQUID IN A ROTATING CYLINDER: PART I. SOLID-BODY ROTATION

C. W. Kitchens, Jr.
N. Gerber
R. Sedney

June 1978

US ARMY ARMAMENT RESEARCH AND DEVELOPMENT COMMAND
BALLISTIC RESEARCH LABORATORY
ABERDEEN PROVING GROUND, MARYLAND

Destroy this report when it is no longer needed.
Do not return it to the originator.

Secondary distribution of this report by originating or sponsoring activity is prohibited.

Additional copies of this report may be obtained from the National Technical Information Service, U.S. Department of Commerce, Springfield, Virginia 22161.

The findings in this report are not to be construed as an official Department of the Army position, unless so designated by other authorized documents.

The use of trade names or manufacturers' names in this report does not constitute indorsement of any commercial product.

REPORT DOCUMENTATION PAGE

READ INSTRUCTIONS BEFORE COMPLETING FORM

1. REPORT NUMBER: TECHNICAL REPORT ARBRL-TR-02081
2. GOVT ACCESSION NO.:
3. RECIPIENT'S CATALOG NUMBER:

4. TITLE (and Subtitle): OSCILLATIONS OF A LIQUID IN A ROTATING CYLINDER: PART I. SOLID-BODY ROTATION

5. TYPE OF REPORT & PERIOD COVERED: Final

6. PERFORMING ORG. REPORT NUMBER:

7. AUTHOR(s):
C. W. Kitchens, Jr.
N. Gerber
R. Sedney

8. CONTRACT OR GRANT NUMBER(s):

9. PERFORMING ORGANIZATION NAME AND ADDRESS:
U.S. Army Ballistic Research Laboratory
(ATTN: DRDAR-BLL)
Aberdeen Proving Ground, MD 21005

10. PROGRAM ELEMENT, PROJECT, TASK AREA & WORK UNIT NUMBERS:
RDT&E 1L161102AH43

11. CONTROLLING OFFICE NAME AND ADDRESS:
U.S. Army Armament Research & Development Command
U.S. Army Ballistic Research Laboratory
(ATTN: DRDAR-BL)
Aberdeen Proving Ground, MD 21005

12. REPORT DATE: JUNE 1978

13. NUMBER OF PAGES: 47

14. MONITORING AGENCY NAME & ADDRESS (if different from Controlling Office):

15. SECURITY CLASS. (of this report): Unclassified

15a. DECLASSIFICATION/DOWNGRADING SCHEDULE:

16. DISTRIBUTION STATEMENT (of this Report)
Approved for public release; distribution unlimited.

17. DISTRIBUTION STATEMENT (of the abstract entered in Block 20, if different from Report)

18. SUPPLEMENTARY NOTES

19. KEY WORDS (Continue on reverse side if necessary and identify by block number)

Disturbance decay rate
Eigenfrequencies
Liquid filled shell
Rotating fluids
Solid-body rotation
Spin-up

20. ABSTRACT (Continue on reverse side if necessary and identify by block number) (lcb)

For application to liquid-filled shell problems, the natural frequencies and decay rates of oscillations of liquids during spin-up in filled rotating cylinders are calculated. In this first part only the fully spun-up flow, i.e., solid-body rotation, is considered. Nevertheless, this part describes in detail the method of solution for the general case of spin-up, and presents results which check with experimental and previous theoretical data closely enough to confirm the reliability of the computational procedure. Data are shown which

(Continued)

20. ABSTRACT (Continued):

illustrate the variation of the eigenfrequencies of a disturbance mode with Reynolds number and aspect ratio of the cylinder. This work treats the viscous perturbation equations for flow of a rotating fluid. An eigenvalue problem results, defined by a sixth-order system which is integrated using the orthonormalization technique.

TABLE OF CONTENTS

I. INTRODUCTION

Projectiles carrying liquid payloads have been flown for at least fifty years[1]. Quite often their flight was erratic because an instability developed due to the presence of the liquid. The work of Stewartson[2] provided an understanding of this phenomenon; he calculated the natural frequencies of free oscillation of a spinning liquid in a cylindrical container and demonstrated that a resonance between these frequencies and the nutational frequency of the projectile causes the instability. This theory and important modifications to it by Wedemeyer[3] have provided rational design methods for liquid-filled projectiles; predictions from these have been verified by range firings and laboratory experiments in which the conditions for the theory were satisfied.

There are three restrictive assumptions in the theory: (i) the amplitude of the disturbance to the rotating fluid is small; (ii) viscous effects are neglected; (iii) the fluid is in solid body rotation. An adequate treatment of large amplitude disturbances is not yet available. Wedemeyer[3] made viscous corrections to Stewartson's theory which considerably extended its usefulness. Relaxing restriction (iii) is the objective of the present work.

The time required for a substantial amount of fluid to achieve solid body rotation is called the spin-up time, t_s. If t_s is small compared to the projectile flight time, Stewartson's assumption (iii) is reasonable, and his theory can be used. The applicability of assumption (iii) depends on the parameters of the projectile-gun system. When (iii) is violated, it is necessary to calculate the frequencies of the liquid during the spin-up phase of its motion. Previous attempts to do this were not successful because of the complexity of the problem.

It is first necessary to know the basic flow during spin-up. The basic theory for this was developed by Wedemeyer[4]; if viscous diffusion

---

1. *Engineering Design Handbook, Liquid-Filled Projectile Design, AMC Pamphlet No. 706-165, U.S. Army Materiel Development and Readiness Command, Washington, D. C., April 1969. AD 853719.*

2. *K. Stewartson, "On the Stability of a Spinning Top Containing Liquid," J. Fluid Mech., Vol. 5, No. 4, September 1959, pp. 577-592.*

3. *E. H. Wedemeyer, "Viscous Corrections to Stewartson's Stability Criterion," BRL Report No. 1325, Aberdeen Proving Ground, Maryland, June 1966. AD 489687.*

4. *E. H. Wedemeyer, "The Unsteady Flow Within a Spinning Cylinder," J. Fluid Mech., Vol. 20, Part 3, 1964, pp. 383-399. Also, see BRL Report No. 1252, Aberdeen Proving Ground, Maryland, October 1963. AD 431846.*

effects are neglected in his model, a simple solution for the spin-up motion is obtained. Although this simple solution is useful for many purposes, it is inadequate for the frequency calculation. We have obtained numerical solutions to the spin-up problem, including viscous diffusion. An efficient program for this is required since the results furnish input to the frequency computation. The latter is accomplished by solving an eigenvalue problem for a sixth-order differential system, the same system of perturbation equations one would obtain in performing a linear stability analysis of the flow.

The Reynolds numbers of interest are large, or Ekman numbers are small, so that the difficulties encountered in solving the eigenvalue problem for the Orr-Sommerfeld equation are present here also. In recent years several techniques have been developed to surmount these difficulties; we choose the orthonormalization technique to solve our eigenvalue problem. Because the perturbation equations have a singularity on the axis, an analytical solution must be obtained there and matched with the numerical solution.

Although the problem of primary interest concerns spin-up, Part I of this report contains only the special case of solid-body rotation, because the authors felt it important to give a detailed description of the numerical procedures yet keep the report a reasonable length. This division is feasible because: (i) the computational method is general, applicable both to solid-body rotation and spin-up flow; (ii) the presentation will not be hampered by complexities which arise in spin-up (e.g., presence of Ekman layers and critical layers, necessity of obtaining basic flows numerically); (iii) checks on the validity of the method can be made with results obtained here. Part II will deal with the spin-up period, treated in a quasi-steady manner so that the same computational method can be used.

II. GOVERNING EQUATIONS AND BOUNDARY CONDITIONS

To calculate the natural frequencies of the spinning liquid we assume a small disturbance to the basic flow. The Navier-Stokes equations for three-dimensional incompressible flow are linearized to give the perturbation equations. If the basic flow is solid-body rotation, the equations can be found in Reference 3; the more general form, for spin-up, is given in References 5 and 6. The non-dimensional flow variables are

---

5. *Y. M. Lynn, "Free Oscillations of a Liquid During Spin-Up," BRL Report No. 1663, Aberdeen Proving Ground, Maryland, August 1973. AD 769710.*

6. *R. Sedney and N. Gerber, "Perturbation Equations for Liquid Spin-Up in Cylindrical Cavities," BRL Technical Report (in preparation).*

$$u \equiv U + \overset{*}{u}, \qquad v \equiv V + \overset{*}{v}, \qquad w \equiv W + \overset{*}{w}, \qquad p \equiv P + \overset{*}{p} \quad , \tag{1}$$

where u, v, and w are total radial, azimuthal, and axial components of velocity, respectively, and p is the pressure. U, V, W, and P are the basic unperturbed variables, and $\overset{*}{u}$, $\overset{*}{v}$, $\overset{*}{w}$, and $\overset{*}{p}$ are the small perturbations in the sense that they are small compared to U, V, W, and P.

The container spin rate is Ω; a is the container radius and c is its half-height; ν is the liquid kinematic viscosity. Length, velocity, pressure, and time are non-dimensionalized by a, $a\Omega$, $\rho\Omega^2a^2$, and Ω^{-1}, respectively, where ρ is the liquid density. Dimensionless, non-rotating, cylindrical coordinates r, θ, and z are used, with z = 0 at one endwall; dimensionless time is denoted by t. For solid-body rotation (the only case considered here) the basic flow is given by

$$U = 0, \qquad V = r, \qquad W = 0, \qquad \partial P/\partial r = r \quad . \tag{2}$$

On substituting (1) and (2) into the Navier-Stokes equations and linearizing, we obtain the perturbation equations:

$$(r\overset{*}{u})_r + \overset{*}{v}_\theta + r\,\overset{*}{w}_z = 0 \tag{3a}$$

$$\overset{*}{u}_t + \overset{*}{u}_\theta - 2\overset{*}{v} = -\overset{*}{p}_r + Re^{-1}\,(\nabla^2\,\overset{*}{u} - r^{-2}\,\overset{*}{u} - 2r^{-2}\,\overset{*}{v}_\theta) \tag{3b}$$

$$\overset{*}{v}_t + \overset{*}{v}_\theta + 2\overset{*}{u} = -r^{-1}\,\overset{*}{p}_\theta + Re^{-1}\,(\nabla^2\,\overset{*}{v} - r^{-2}\,\overset{*}{v} + 2\,r^{-2}\,\overset{*}{u}_\theta) \tag{3c}$$

$$\overset{*}{w}_t + \overset{*}{w}_\theta = -\overset{*}{p}_z + Re^{-1}\,\nabla^2\,\overset{*}{w} \tag{3d}$$

where subscripts denote partial derivatives,

$$\nabla^2 \equiv \partial^2/\partial r^2 + r^{-1}\,\partial/\partial r + r^{-2}\,\partial^2/\partial\theta^2 + \partial^2/\partial z^2 \quad , \tag{4}$$

and the Reynolds number is

$$Re = \Omega\, a^2/\nu \quad . \tag{5}$$

We assume that the disturbance can be expressed as a superposition of modes; i.e., a triple Fourier expansion of the disturbances in θ, z, and t, with coefficients functions of r:

$$\overset{*}{u} = \hat{u}\,(r)\,\cos Kz\,\exp\,[i\,(Ct - m\theta)] \tag{6a}$$

$$\overset{*}{v} = \hat{v}\,(r)\,\cos Kz\,\exp\,[i\,(Ct - m\theta)] \tag{6b}$$

$$\overset{*}{w} = \hat{w}\,(r)\,\sin Kz\,\exp\,[i\,(Ct - m\theta)] \tag{6c}$$

$$\overset{*}{p} = \hat{p}\,(r)\,\cos Kz\,\exp\,[i\,(Ct - m\theta)] \tag{6d}$$

where

$$K = k\pi/(2c) \quad . \tag{7}$$

In this form the disturbances are complex, the real parts being the physical quantities; also the functions $\hat{u}(r)$, $\hat{v}(r)$, $\hat{w}(r)$, and $\hat{p}(r)$ are complex. The integers $m = 0, \pm 1, \ldots$, and $k = 1, 2, \ldots$ are azimuthal and axial wave numbers, respectively; m expresses the condition that the disturbance is periodic in the interval $0 \leqslant \theta \leqslant 2\pi$. The non-dimensional quantity $C \equiv C_R + i\,C_I$ is the eigenvalue we seek to determine. The natural frequency is equal to $C_R\Omega$ and the decay rate of the disturbance is equal to $C_I\Omega$.

The boundary conditions at the end walls ($z = 0, 2c$) are $\overset{*}{u} = \overset{*}{v} = \overset{*}{w} = 0$. The form assumed in (6) allows only the condition of zero velocity normal to the wall, $\overset{*}{w} = 0$, to be satisfied. However, the modal decomposition, or separation of variables, requires the trigonometric functions; consequently, the no-slip condition on the endwalls, $\overset{*}{u} = \overset{*}{v} = 0$, is not satisfied. A boundary layer type of correction is made to the solution to account for this. This correction, described in Appendix A, is analogous to that made by Wedemeyer at both the sidewall and endwalls. The correction has a significant effect on C_I.

When $\overset{*}{u}$, $\overset{*}{v}$, $\overset{*}{w}$, and $\overset{*}{p}$ from (6) are substituted into (3), a set of homogeneous linear ordinary differential equations is obtained for $\hat{u}$, $\hat{v}$, $\hat{w}$, $\hat{p}$. These must be converted to canonical form to be integrated numerically; i.e.,

$$y_i' \equiv dy_i/dr = f_i\,(r, y_1, y_2, \ldots y_6), \qquad i = 1,2 \ldots 6\ ,$$

where

$$\begin{aligned} y_1 &= \hat{u} & y_3 &= \hat{v}' & y_5 &= \hat{w}' \\ y_2 &= \hat{u} - i\,\hat{v} & y_4 &= \hat{w} & y_6 &= \hat{p}\ . \end{aligned} \tag{8}$$

The form for y_2 is convenient for satisfying boundary conditions. After the required manipulations are performed the following sixth order system of equations is obtained:

$$y_1' = (m - 1)\, r^{-1}\, y_1 - m\, r^{-1}\, y_2 - K\, y_4 \tag{9a}$$

$$y_2' = (m - 1)\, r^{-1}\, y_1 - m\, r^{-1}\, y_2 - i\, y_3 - K\, y_4 \tag{9b}$$

$$y_3' = 2\,(Re + i\, mr^{-2})\, y_1 + i\,(B + r^{-2})(y_2 - y_1) - r^{-1}\, y_3 - i\, m\, Re\, r^{-1}\, y_6 \tag{9c}$$

$$y_4' = y_5 \tag{9d}$$

$$y_5' = B\, y_4 - r^{-1}\, y_5 - K\, Re\, y_6 \tag{9e}$$

$$y_6' = -Re^{-1}\, B\, y_1 + i\, Re^{-1}\,(2\, Re + i\, m\, r^{-2})(y_2 - y_1) + i\, m\, Re^{-1}\, r^{-1}\, y_3 - K\, Re^{-1}\, y_5 \tag{9f}$$

where

$$B = (m^2/r^2) + K^2 + i\, Re\,(C - m) \quad .$$

The terminal conditions at the sidewall ($r = 1$) are $\hat{u}(1) = \hat{v}(1) = \hat{w}(1) = 0$, or

$$y_1(1) = y_2(1) = y_4(1) = 0 \quad . \tag{10}$$

The initial conditions depend on the particular problem being solved. For a filled cylinder with an inner concentric rod, or central burster, the no-slip conditions apply at the inner wall, $r = b$:

$$y_1(b) = y_2(b) = y_4(b) = 0 \quad . \tag{11}$$

For a filled cylinder with no inner rod the inner boundary is r = 0, and the boundary conditions[6] depend on the azimuthal wave number:

$$m = 0: \quad y_1(0) = y_2(0) = y_5(0) = 0 \tag{12a}$$

$$m = 1: \quad y_2(0) = y_4(0) = y_6(0) = 0 \tag{12b}$$

$$m > 1: \quad y_1(0) = y_2(0) = y_4(0) = 0 \ . \tag{12c}$$

Their derivation requires only kinematics and single-valuedness (see Batchelor, E.K. and Gill, A.E., J. Fluid Mech. 14, 529).

The wave numbers m and k are assigned, and the values of c and Re are given. Then (9), (10), and (11) or (12) constitute an eigenvalue problem. The radial modes are designated by the integers n = 1, 2, ...

III. NUMERICAL PROCEDURE FOR SOLVING EIGENVALUE PROBLEM

The eigenvalue problem defined by the sixth-order system (9), (10), and (11) or (12) bears some similarity to the Orr-Sommerfeld equation. In particular the coefficient of the highest derivative contains Re^{-1}; in liquid-filled shell applications values of $Re \sim 10^6$ are commonplace. Our numerical procedure uses one of the methods developed for solving numerically the Orr-Sommerfeld equation, viz., orthonormalization.

A. Method of Superposition

An outline of the method will be given after a more compact notation is introduced. Matrices will be denoted by upper case, underscored symbols. Express (9)-(12) in matrix form:

$$\underline{Y}' = \underline{Y}(r)\ \underline{G} \tag{13}$$

$$\underline{Y}(b)\ \underline{E} = \underline{0} \tag{14}$$

$$\underline{Y}(1)\ \underline{F} = \underline{0} \tag{15}$$

where $\underline{Y}$ is the solution vector $\underline{Y} = \{y_1, \ldots, y_6\}$, a 1 x 6 matrix. $\underline{G}$ is a 6 x 6 matrix; $\underline{E}$ and $\underline{F}$ are 6 x 3 matrices the elements of which are obtained from (9)-(12); b is the radial coordinate where initial conditions are specified. The elements of $\underline{E}$ depend on the choice of boundary conditions (11) or (12). Each of the three columns of $\underline{E}$ and $\underline{F}$ has only one non-zero element.

The general solution of (13) can be expressed as a linear combination of six linearly independent solutions. If these are chosen so that (14) is satisfied, then only three independent solutions are available. These are denoted by

$$\underline{S}_j(r) = \{s_{j1}, \ \ldots \ s_{j6}\} \qquad j = 1, 2, 3,$$

so that the solution can be expressed as

$$\underline{Y}(r) = \underline{\Gamma} \ \underline{S} = \gamma_1 \underline{S}_1 + \gamma_2 \underline{S}_2 + \gamma_3 \underline{S}_3 \tag{16}$$

where $\underline{S}$ is a 3 x 6 matrix whose rows are the vectors $\underline{S}_j$, and $\underline{\Gamma} = \{\gamma_1, \gamma_2, \gamma_3\}$ is a 1 x 3 matrix of constant coefficients. Note that (14) can be written as

$$\underline{Y}(b) \ \underline{E} = \underline{\Gamma} \ \underline{S}(b) \ \underline{E} = \underline{0}$$

or

$$\underline{S}(b) \ \underline{E} = \underline{0} \ . \tag{17}$$

The eigenvalue problem is solved by iteration. A value for C is selected at each stage of the iteration and one integration pass is made between r = b and r = 1 for each of the three independent solutions, $\underline{S}_1$, $\underline{S}_2$, and $\underline{S}_3$, giving the $s_{ji}(1)$, j = 1, 2, 3 and i = 1, ..., 6. From (15)

$$\underline{Y}(1) \ \underline{F} = \underline{\Gamma} \ \underline{S}(1) \ \underline{F} = \underline{0} \ . \tag{18}$$

A non-trivial solution for $\underline{\Gamma}$ requires

$$D(C) \equiv \text{Det} \ [\underline{S}(1) \ \underline{F}] = 0 \ . \tag{19}$$

The iteration process provides a systematic method of choosing the values of C used in the numerical integration of (9) until (19) is satisfied to within a specified accuracy. At each stage of the iteration $\underline{\Gamma}$ is obtained by solving (18); finally the eigenfunctions are found from (16).

The method of superposition described above cannot be carried out successfully for large values of Re. The initially linearly-independent solutions, $\underline{S}_1$, $\underline{S}_2$, and $\underline{S}_3$, become numerically dependent during the

numerical integration. The determinant in (19) then generally fails to yield a clear-cut root, C, and the iterative process does not converge. This occurs because one or more of the solutions grows rapidly with r, yielding numbers of higher orders of magnitude than the other solutions. A method of orthonormalization is employed in this work to maintain linear independence and reasonable order-of-magnitude solutions. The technique which we adopt is based on a version of Godunov's procedure[7] described by Conte[8].

B. Numerical Integration and Orthonormalization

The linear independence of the solutions can be maintained by the orthogonalization process described below. The solutions can be further conditioned by periodically renormalizing them, thus preventing any of them from growing inordinately large. Procedures to test the solution vectors for loss of independence are available[9]; however, to avoid unduly complicating the computer program, we specify the number and locations of orthonormalizations.

The integration procedure starts with orthonormal initial values (discussed in next section) specified for s_{ji} at $r = \varepsilon$. When $b = 0$, an analytical solution near $r = 0$ must be used to obtain the solution vectors at the "matching radius" ε; when $b \neq 0$, the value of ε is taken equal to b.

The numerical integration of (9) is carried out over the interval $\varepsilon \leqslant r \leqslant 1$ using a fourth-order Runge-Kutta technique. This interval is divided into N subintervals of equal length, $(1 - \varepsilon)/N$. At the end of each subinterval the solution vectors are orthonormalized using the Gram-Schmidt process. At the end of the λth subinterval there are three solution vectors $\underline{S}_1^{\lambda}$, $\underline{S}_2^{\lambda}$, and $\underline{S}_3^{\lambda}$, where $\lambda = 1, \ldots, N$ denotes the subinterval index. For the complex solution vectors we define a non-standard inner product

$$\underline{S}_1 \cdot \underline{S}_2 \equiv \sum_{i=1}^{6} s_{1i}\, s_{2i} \quad .$$

7. *S. Godunov, "On the Numerical Solution of Boundary-Value Problems for Systems of Linear Ordinary Differential Equations,"* Uspekhi Mat. Nauk., *Vol. 16, 1961, pp. 171-174.*

8. *S. D. Conte, "The Numerical Solution of Linear Boundary Value Problems,"* SIAM Review, *Vol. 8, 1966, pp. 309-321.*

9. *M. R. Scott and H. A. Watts, "SUPORT-A Computer Code for Two-Point Boundary-Value Problems via Orthonormalization," Sandia Laboratories Report SAND 75-0198, Albuquerque, New Mexico, June 1975, pp. 89-94.*

The two vectors are orthogonal when $\underline{S}_1 \cdot \underline{S}_2 = 0$. The norm of a vector is defined by

$$\left|\left|\underline{S}\right|\right|^2 = \underline{S} \cdot \underline{S} \quad .$$

This inner-product was used by Davey[10]; it has the advantage that the solutions are analytic functions of C, a useful property in the iteration process. It has the disadvantage that the norm can be zero for a non-zero vector; however, this difficulty has never arisen.

The new set of orthogonal vectors, denoted by $\overline{\underline{S}}_1$, $\overline{\underline{S}}_2$, and $\overline{\underline{S}}_3$, is obtained using the following transformation:

$$\overline{\underline{S}}^{\lambda} = \underline{A}^{\lambda}\ \underline{S}^{\lambda} \tag{20}$$

where $\underline{A}^{\lambda}$ is a 3 x 3 matrix whose elements α_{ij} are given by

$$\alpha_{11}^{\lambda} = \alpha_{22}^{\lambda} = \alpha_{33}^{\lambda} = 1$$

$$\alpha_{21}^{\lambda} = \alpha_{31}^{\lambda} = \alpha_{32}^{\lambda} = 0$$

$$\alpha_{12}^{\lambda} = Q^{\lambda}\ [(\underline{S}_3^{\lambda} \cdot \underline{S}_3^{\lambda})(\underline{S}_1^{\lambda} \cdot \underline{S}_2^{\lambda}) - (\underline{S}_3^{\lambda} \cdot \underline{S}_1^{\lambda})(\underline{S}_3^{\lambda} \cdot \underline{S}_2^{\lambda})] \tag{21}$$

$$\alpha_{13}^{\lambda} = Q^{\lambda}\ [(\underline{S}_3^{\lambda} \cdot \underline{S}_1^{\lambda})(\underline{S}_2^{\lambda} \cdot \underline{S}_2^{\lambda}) - (\underline{S}_3^{\lambda} \cdot \underline{S}_2^{\lambda})(\underline{S}_1^{\lambda} \cdot \underline{S}_2^{\lambda})]$$

$$\alpha_{23}^{\lambda} = -\ (\underline{S}_2^{\lambda} \cdot \underline{S}_3^{\lambda})\ /\ (\underline{S}_3^{\lambda} \cdot \underline{S}_3^{\lambda}) \quad ,$$

where

$$Q^{\lambda} = 1/[(\underline{S}_3^{\lambda} \cdot \underline{S}_2^{\lambda})^2 - (\underline{S}_2^{\lambda} \cdot \underline{S}_2^{\lambda})(\underline{S}_3^{\lambda} \cdot \underline{S}_3^{\lambda})] \quad .$$

The solution vectors are then normalized, forming three orthonormal basis vectors $\underline{T}_j^{\lambda}$ (j = 1, 2, 3). The complete orthonormalization process can be expressed as

10. *A. Davey, "A Simple Numerical Method for Solving Orr-Sommerfeld Problems," Quarterly Journal of Mathematics and Applied Mechanics, Vol. 26, Part 4, 1973, pp. 401-411.*

$$\underline{T}^{\lambda} = \underline{B}\,\underline{S}^{\lambda} \quad . \tag{22}$$

The elements of $\underline{T}^{\lambda}$ are denoted by t^{λ}_{ji}; the elements of the matrix $\underline{B}^{\lambda}$ are

$$\beta^{\lambda}_{11} = 1/\left|\left|\underline{\bar{S}}^{\lambda}_{1}\right|\right| , \qquad \beta^{\lambda}_{22} = 1/\left|\left|\underline{\bar{S}}^{\lambda}_{2}\right|\right| , \qquad \beta^{\lambda}_{33} = 1/\left|\left|\underline{\bar{S}}^{\lambda}_{3}\right|\right|$$

$$\beta^{\lambda}_{21} = \beta^{\lambda}_{31} = \beta^{\lambda}_{32} = 0 , \qquad \beta^{\lambda}_{12} = \alpha^{\lambda}_{12}/\left|\left|\underline{\bar{S}}^{\lambda}_{1}\right|\right| \tag{23}$$

$$\beta^{\lambda}_{13} = \alpha^{\lambda}_{13}/\left|\left|\underline{\bar{S}}^{\lambda}_{1}\right|\right| , \qquad \beta^{\lambda}_{23} = \alpha^{\lambda}_{23}/\left|\left|\underline{\bar{S}}^{\lambda}_{2}\right|\right| \quad .$$

The three solutions $\underline{T}^{\lambda}_{j}$ are evaluated at the end of the λth subinterval and taken as initial values of $\underline{S}^{\lambda+1}_{j}$ for the continuation of the numerical integration into the $(\lambda + 1)$st subinterval. This process of integration and orthonormalization is carried out for each successive subinterval, finally yielding three orthonormal basis vectors $\underline{T}^{N}_{j}(1)$.

C. Initial and Terminal Conditions

The initial conditions of $r = \varepsilon$ must be selected so that the boundary conditions, (11) or (12), are satisfied. For a cylinder with an inner concentric rod the initial conditions at $r = \varepsilon$ are taken to be

$$\underline{S}_1(\varepsilon) = \{0,0,1,0,0,0\} , \qquad \underline{S}_2(\varepsilon) = \{0,0,0,0,1,0\}$$

$$\underline{S}_3(\varepsilon) = \{0,0,0,0,0,1\} . \tag{24}$$

These orthonormal vectors satisfy (11), or equivalently, (17).

For a cylinder with no inner rod boundary conditions (12) are specified at $r = 0$. The integration of (9) must be carried out in two stages because the inverse powers of r prevent direct numerical integration from $r = 0$. The procedure we adopt is to obtain three linearly independent analytical solutions near the axis which satisfy (12) at $r = 0$. Numerical values of these solutions at the matching radius $r = \varepsilon$ are used as initial conditions for numerical integration over the interval $\varepsilon \leqslant r \leqslant 1$. The analytical solutions are obtained from power series expansions for $\hat{u}$, $\hat{v}$, $\hat{w}$, and $\hat{p}$ using the method of undetermined coefficients to obtain recursion formulas. The power series coefficients for $m = 1$ are presented in Appendix B. There are three arbitrary

coefficients (b_o, d_1, e_1), which are specified so as to give three independent solutions. Terminal conditions (10) lead to (19), modified by orthonormalization so that $\underline{T}(1)$ replaces $\underline{S}(1)$. In terms of $\underline{T}(1)$ the following equation must be solved for C:

$$D(C) \equiv \begin{vmatrix} t_{11}^N(1) & t_{21}^N(1) & t_{31}^N(1) \\ t_{12}^N(1) & t_{22}^N(1) & t_{32}^N(1) \\ t_{14}^N(1) & t_{24}^N(1) & t_{34}^N(1) \end{vmatrix} = 0 \quad . \tag{25}$$

Once a solution to (25) has been found, γ_1, γ_2, and γ_3 of (16) can be determined to within a constant multiple. The matrix from which the determinant in (25) originates is generally of rank 2. Thus, we set $\gamma_3=1$ so that γ_1 and γ_2 are found from

$$\begin{aligned} t_{11}^N(1)\ \gamma_1 + t_{21}^N(1)\ \gamma_2 &= -\ t_{31}^N(1) \\ t_{12}^N(1)\ \gamma_1 + t_{22}^N(1)\ \gamma_2 &= -\ t_{32}^N(1) \ . \end{aligned} \tag{26}$$

D. Iteration Procedure to Solve for Eigenvalue

An eigenvalue $C \equiv C_R + iC_I$ is a root of (25), which is equivalent to the following system of two real equations:

$$D_R(C_R,C_I) = 0 \ , \qquad D_I(C_R,C_I) = 0 \ , \tag{27}$$

where D_R and D_I are real and imaginary parts of D. This system is solved by a method of successive iteration. An initial guess C_1 is assumed which must be reasonably close to the solution because of the sensitivity of D_R and D_I to variations in C_R and C_I. An iteration operator, J, is applied to C_1 yielding a new estimate C_2, etc. A sequence of iterates is determined from

$$C_{\mu+1} = J\ (C_\mu) \quad .$$

When (25) is satisfied and $|C_{\mu+1} - C_\mu|$ is small to within specified tolerances, for some μ, the iteration is stopped. We found it advisable to satisfy both requirements since the condition on C could sometimes be satisfied without the one on D being satisfied.

The iteration operation used here is an extension of Newton's method. For small changes in C and D between the μth and $(\mu+1)$st iterations we can write

$$\begin{aligned} D_{R_{\mu+1}} - D_{R_\mu} &= (\partial D_R/\partial C_R)\,[C_{R_{\mu+1}} - C_{R_\mu}] + (\partial D_R/\partial C_I)\,[C_{I_{\mu+1}} - C_{I_\mu}] \\ D_{I_{\mu+1}} - D_{I_\mu} &= (\partial D_I/\partial C_R)\,[C_{R_{\mu+1}} - C_{R_\mu}] + (\partial D_I/\partial C_I)\,[C_{I_{\mu+1}} - C_{I_\mu}] \,. \end{aligned} \tag{28}$$

The partial derivatives are approximated by

$$\begin{aligned} \partial D_R/\partial C_R &= [D_R\,(C_{R_\mu} + \Delta C_R, C_{I_\mu}) - D_R\,(C_{R_\mu}, C_{I_\mu})]/\Delta C_R \\ \partial D_R/\partial C_I &= [D_R\,(C_{R_\mu}, C_{I_\mu} + \Delta C_I) - D_R\,(C_{R_\mu}, C_{I_\mu})]/\Delta C_I \,, \end{aligned} \tag{29}$$

with similar expressions for $\partial D_I/\partial C_R$ and $\partial D_I/\partial C_I$. Appropriate small values for ΔC_R and ΔC_I are used, e.g. $\Delta C_R = \ell\, C_R$ unless C_R is small, in which case $C_R = \ell$; ℓ is an input parameter, typically $\ell = 0.001$. The goal of each iteration is to make $D_{\mu+1}$ vanish. We set $D_{R_{\mu+1}} = D_{I_{\mu+1}} = 0$ in (28) and thereby get formulas for $C_{R_{\mu+1}}$ and $C_{I_{\mu+1}}$ in terms of C_{R_μ} and C_{I_μ}.

A simplification is possible at this point, since, with the chosen definition of inner product, D(C) is an analytic function of C which satisfies the Cauchy-Riemann conditions:

$$\partial D_R/\partial C_R = \partial D_I/\partial C_I \,, \qquad \partial D_R/\partial C_I = -\,\partial D_I/\partial C_R \,. \tag{30}$$

We substitute (30) into (28) (with $D_{\mu+1} = 0$) and obtain the operator $J(C_\mu)$ as the solution to the set of equations:

$$(\partial D_R/\partial C_R)\, C_{R_{\mu+1}} - (\partial D_I/\partial C_R)\, C_{I_{\mu+1}} = H_1\,(C_\mu, D_\mu)$$
$$(\partial D_I/\partial C_R)\, C_{R_{\mu+1}} + (\partial D_R/\partial C_R)\, C_{I_{\mu+1}} = H_2\,(C_\mu, D_\mu) \qquad (31)$$

where

$$H_1\,(C_\mu, D_\mu) \equiv (\partial D_R/\partial C_R)\, C_{R_\mu} - (\partial D_I/\partial C_R)\, C_{I_\mu} - D_{R_\mu}$$
$$H_2\,(C_\mu, D_\mu) \equiv (\partial D_I/\partial C_R)\, C_{R_\mu} + (\partial D_R/\partial C_R)\, C_{I_\mu} - D_{I_\mu} \qquad (32)$$

Since (31) and (32) contain only partial derivatives with respect to C_R, $D_R\,(C_{R_\mu}, C_{I_\mu} + \Delta C_I)$ in (29) and $D_I\,(C_{R_\mu}, C_{I_\mu} + \Delta C_I)$ in the expression for $\partial D_I/\partial C_I$ need not be evaluated. Practically, this cuts the required computer time almost in half since only six integration passes (two for each of the three independent solutions) are needed per iteration, versus the twelve that would be required if D(C) were not analytic.

E. Evaluation of Eigenfunctions

For some applications we may also wish to evaluate the flow variable perturbations $\hat{u}(r)$, $\hat{v}(r)$, $\hat{w}(r)$, and $\hat{p}(r)$, or, equivalently, $\underline{Y}(r) \equiv \{y_1, \ldots, y_6\}$, the eigenfunctions associated with the eigenvalue C. The solution $\underline{Y}$ is expressed as a combination of the three linearly independent solutions, according to (16). Because of the orthonormalization at the end of each subinterval the constants in (16) are different for each subinterval: γ_1^λ, γ_2^λ, γ_3^λ. The solutions $\underline{S}_1(r)$, $\underline{S}_2(r)$, and $\underline{S}_3(r)$ are computed over each subinterval and stored; the evaluation of the eigenfunctions reduces to the problem of determining γ_1^λ, γ_2^λ, and γ_3^λ.

At the $(\lambda - 1)$st junction point $r_{\lambda-1} = \varepsilon + (1 - \varepsilon)(\lambda - 1)/N$ and the solution is

$$\underline{Y}^{\lambda-1}\,(r_{\lambda-1}) = \underline{\Gamma}^{\lambda-1}\, \underline{S}^{\lambda-1}\,(r_{\lambda-1}) \qquad (33)$$

The initial value of the solution in the λth subinterval is (see Section III.B)

$$\underline{Y}^{\lambda}(r_{\lambda-1}) = \underline{\Gamma}^{\lambda}\,\underline{T}^{\lambda-1}(r_{\lambda-1}) \quad . \tag{34}$$

At each junction point $\underline{S}^{\lambda} = \underline{T}^{\lambda-1}$ and

$$\underline{S}^{\lambda} = \underline{B}^{\lambda-1}\,\underline{S}^{\lambda-1}$$

from (22). The elements of the matrix $\underline{B}^{\lambda-1}$, given by (23), are stored for all subintervals during each iteration. Continuity requires that $\underline{Y}^{\lambda-1}(r_{\lambda-1}) = \underline{Y}^{\lambda}(r_{\lambda-1})$. Equating the right-hand sides of (33) and (34) gives

$$\underline{\Gamma}^{\lambda-1}\,\underline{S}^{\lambda-1}(r_{\lambda-1}) = \underline{\Gamma}^{\lambda}\,\underline{B}^{\lambda-1}\,\underline{S}^{\lambda-1}(r_{\lambda-1})$$

or

$$\underline{\Gamma}^{\lambda-1} = \underline{\Gamma}^{\lambda}\,\underline{B}^{\lambda-1} \quad , \tag{35}$$

which is used to calculate the $\underline{\Gamma}^{\lambda-1}$ from known $\underline{\Gamma}^{\lambda}$. At the last (Nth) subinterval γ_1^N, γ_2^N, and γ_3^N are known. In our procedure $\gamma_3^N = 1$, and γ_2^N and γ_3^N are obtained from (26). The γ_j^{N-1} (j = 1,2,3) are found using (35), and so forth, down to $\lambda = 2$. The appropriate linear combinations of $\underline{S}_1$, $\underline{S}_2$, and $\underline{S}_3$ are evaluated in each subinterval to give the eigenfunctions over the interval $\varepsilon \leqslant r \leqslant 1$.

F. Additional Aspects of the Computation

As mentioned in Section III.D, convergence of the iteration process requires that the initial guess for the eigenvalue C be reasonably close to the actual value, say within 10%; typically, convergence criteria are satisfied in five or less iterations. For solid body rotation and m = 1, satisfactory trial values can be obtained from Wedemeyer's simple formulae for eigenvalues[1,3] obtained by applying a viscous correction (described in Section IV) to Stewartson's results[2]. In fact, the latter can also be used for the initial guess, with $C_I = 0$ because the perturbation is inviscid. The C_R are given in tabular form in Reference 1 for given c and k and radial mode numbers n = 1, 2, 3. (In Reference 1, C_R is denoted by τ_o, and 2j = k - 1.) The value of n is the maximum number of (non-boundary) zeros in the real and imaginary

parts of the set of $\hat{u}$, $\hat{v}$, $\hat{w}$, and $\hat{p}$. A typical solution is illustrated in Figure 1*, which shows the real part of $\hat{p}(r)$ for the lowest two radial modes for the case c = 3.148, Re = 8977, k = 3, m = 1. The number of zeros is n - 1 here, but for $\hat{v}$ the number of zeros is n.

In Figure 2 the real part of $\hat{w}$ is plotted to demonstrate the presence of the boundary layer on the sidewall.

It was stated in Section III.C that three independent analytic solutions to (9) were obtained near r = 0. Though it has not been proven, it is fairly certain that any other independent solution would be singular at r = 0, and thus inadmissable. For m = 1 we obtain three independent solutions by choosing the complex constants b_o, d_1, and e_1 in Appendix B in the following way: during each iteration $\{b_o, d_1, e_1\}$ is equal to {1,0,0} for the first integration pass, {0,1,0} for the second pass, and {0,0,1} for the third. Approximately ten terms of the series are used to approximate the functions for $\varepsilon = 0.001$. The actual number of terms used is adjusted to insure that the series converge with a difference between successive partial sums of no greater than typically 1×10^{-6}.

Since m = 1 modes are the only ones which lead to an overturning moment on the projectile, only these will be considered in this report. However, other modes, particularly m = 0, have also been computed.

IV. ENDWALL BOUNDARY CONDITION CORRECTION

The technique described in Sections II and III will provide natural frequencies within the limitations of the linearized theory. However, as pointed out in Section II, in order to perform a modal analysis in the longitudinal direction it is necessary to abandon the no-slip boundary conditions $\overset{*}{u} = \overset{*}{v} = 0$ on the endwalls; only $\overset{*}{w} = 0$ could be satisfied. The perturbation velocities thus satisfy the inviscid boundary conditions. Because these incorrect boundary conditions have a significant effect on C_I a correction was devised, analogous to Wedemeyer's viscous correction[1,3] to Stewartson's inviscid results. This correction is briefly described here; details are given in Appendix A.

Experiments with a liquid-filled gyrostat revealed discrepancies between observations and Stewartson's inviscid analysis. To account for these Wedemeyer analyzed the perturbation boundary layers along the sidewall and endwalls. He concluded that the viscous flow problem is equivalent to an inviscid problem with boundary conditions

---

* Figures 1 and 2 are located on page 26.

$$\overset{*}{u} = 0 \qquad \text{at} \qquad r = 1 - \delta a_w$$

$$\overset{*}{w} = 0 \qquad \text{at} \qquad z = \delta c_w \qquad \text{and} \qquad z = (2c - \delta c_w) \quad , \tag{36}$$

where δa_w and δc_w are non-dimensional displacement thicknesses for the sidewall and endwall boundary layers, respectively. The complex quantities δa_w and δc_w are algebraic functions of Re and the inviscid C_R but are independent of r, θ, and t. The analysis is applicable for large Re (but not so large as to cause boundary layer instabilities). Large Re requires that $|\delta a_w| \ll 1$ and $|\delta c_w| \ll 1$, conditions which are generally true for $Re > 10^3$. Solving the inviscid problem with (36) modifies the eigenfrequency by a small complex increment. The resulting frequency and damping rate agree with experimental observations.

In our analysis the viscous diffusion terms are present in the perturbation equations. The correction is needed here because conditions $\overset{*}{u} = \overset{*}{v} = 0$ on $z = 0$, $2c$ are not satisfied. This correction, in principle, is different from Wedemeyer's; but after proper formulation the analysis proceeds in much the same way. A sidewall correction is not required since the perturbation solution satisfies the no-slip conditions at $r = 1$. A boundary layer analysis is made on the difference between the flows with and without the no-slip conditions on the endwalls, and a displacement thickness δc_s is obtained which has the same properties as δc_w. When $C_I = 0$, $\delta c_s = \delta c_w$. The eigenvalue problem is solved again, now using the modified complex half-height, $c - \delta c_s$. No computational difficulties are introduced because δc_s directly affects only K in (7), which appears in the already complex (9). The effects of this correction on C_R and C_I are discussed in Section V.

V. DESCRIPTION OF NUMERICAL RESULTS

A program as extensive as the eigenvalue computation program requires checks to establish its reliability. Three types of checks will be treated: (a) related problems for which results are available in the literature; (b) Wedemeyer's approximate solution to the eigenvalue problem; (c) experimental data.

A. Check With Flow Between Rotating Cylinders

Many investigations have been carried out on the stability of flow between concentric rotating cylinders, often called Taylor's problem; when the flow is unstable Taylor vortices are generated. The basic flow is steady but not solid-body rotation because the angular

velocities of the two cylinders differ. V(r) has r and r^{-1} terms, and is independent of z for infinite length cylinders. Since our program is written for general V(r), eigenvalues can be calculated for the two-cylinder problem.

The first comparison is made with a result in Reference 11 for which the parameters are Re = 796.8, b = 0.70, Ω_b/Ω_a = -1, K = 13.280, and m = 2, where b is the non-dimensional radius of the inner cylinder, and Ω_b and Ω_a are the dimensional angular velocities of the inner and outer cylinders, respectively. The computed eigenvalue is C_R = 0.6763 and C_I = -0.0007, compared to C_R = 0.6759 and C_I = 0.0000 in Reference 11. The second comparison is made with a result of Reference 12 for Re = 4270.2, b = .9512, Ω_b/Ω_a = 0, K = 64.10, and m = -1. Values of C_R = -0.5141 and C_I = -0.1443 are obtained both from our program and from Reference 12. The agreement between our results and those of References 11 and 12 lends support to the validity of all of them.

B. Check With Wedemeyer's Solution and Parametric Study of Eigenvalues

No previous viscous perturbation calculations exist, but Wedemeyer's viscous correction to the Stewartson theory provides an approximate solution to the eigenvalue problem which agrees well with experiment. Therefore, results from his theory will be compared with ours; a sufficient number of cases will be presented to exhibit the variation of the eigenvalue with Re and c.

Tables 1-3 provide the eigenvalues for the m = 1, k = 3, n = 1 mode over the ranges c = 3, 4, 5 and Re = 10^3, 10^4, 10^5, and 10^6. The endwall displacement thicknesses δc_w and δc_s are also presented; there is no reason for these two quantities to be the same; but in fact they differ at most by a few percent. The effect of the boundary condition correction on C_R and C_I is demonstrated in these tables. Except for c = 3 and the two smaller Re, the percentage correction to C_I is much larger than that to C_R. With boundary condition correction the C_R differ from Wedemeyer's results by a few percent at most for all cases. However, for the three aspect ratios and Re = 10^3 and 10^4 the differences

---

11. *E. R. Krueger, A. Gross, and R. C. DiPrima, "On the Relative Importance of Taylor-Vortex and Non-Axisymmetric Modes in Flow Between Rotating Cylinders," J. Fluid Mech., (1966), Vol. 24, Part 3, pp. 521-538.*

12. *P. M. Eagles, "On Stability of Taylor Vortices by Fifth-Order Amplitude Expansions," J. Fluid Mech., (1971), Vol. 49, Part 3, pp. 529-550.*

in C_I are greater than 10%, and for c = 5, Re = 10^3 it is 43%. In principle, our results should be more accurate since no correction is needed at the sidewall and viscous diffusion effects in the interior are included. Whether or not this is the case requires a comparison with experiment (or perhaps a full numerical solution to the perturbation problem). On the basis of the following discussion it is concluded that sufficient experimental evidence to discriminate between Wedemeyer's results and ours does not exist.

Table 1. Eigenvalues and Half-Height Corrections for Solid-Body Rotation: m = 1, k = 3, n = 1, c = 3.

Re = $a^2\Omega/\nu$	δc_w	δc_s	$C_{R_{Wed.}}$	B.C. Correction C_R	No B.C. Correction C_R	$C_{I_{Wed.}}$	B.C. Correction C_I	No B.C. Correction C_I
10^6	.000855- .00127 i	.000856- .00127 i	.00472	.00484	.00509	.000996	.00100	.000630
10^5	.00270- .00401 i	.00271- .00401 i	.00553	.00564	.00643	.00315	.00324	.00207
10^4	.00855- .01267 i	.00858- .01273 i	.00808	.00815	.01066	.00996	.01100	.00727
10^3	.02705- .04008 i	.02754- .04069 i	.01614	.01578	.02382	.03150	.04256	.03052

Table 2. Eigenvalues and Half-Height Corrections for Solid-Body Rotation: m = 1, k = 3, n = 1, c = 4.

Re = $a^2\Omega/\nu$	δc_w	δc_s	$C_{R_{Wed.}}$	B.C. Correction C_R	No B.C. Correction C_R	$C_{I_{Wed.}}$	B.C. Correction C_I	No B.C. Correction C_I
10^6	.000805- .00150 i	.000806- .00151 i	.24352	.24375	.24390	.000915	.000927	.000636
10^5	.00255- .00476 i	.00256- .00477 i	.24454	.24475	.24525	.00289	.00300	.00208
10^4	.00805- .01505 i	.00815- .01515 i	.24775	.24797	.24953	.00915	.01024	.00731
10^3	.02547- .04758 i	.02685- .04859 i	.25793	.25772	.26277	.02894	.03995	.03051

Table 3. Eigenvalues and Half-Height Corrections for Solid-Body Rotation: m = 1, k = 3, n = 1, c = 5.

Re $= a^2\Omega/\nu$	δc_w	δc_s	$C_{R_{Wed.}}$	B.C. Correction C_R	No B.C. Correction C_R	$C_{I_{Wed.}}$	B.C. Correction C_I	No B.C. Correction C_I
10^6	.000783- .00181 i	.000784- .00181 i	.40225	.40227	.40237	.000822	.000837	.000602
10^5	.00248- .00573 i	.00249- .00574 i	.40330	.40333	.40364	.00260	.00272	.00198
10^4	.00783- .01811 i	.00800- .01827 i	.40664	.40666	.40768	.00822	.00935	.00699
10^3	.02476- .05727 i	.02723- .05875 i	.41719	.41674	.42010	.02600	.03729	.02966

C. Check With Experimental Data

This check is the most useful one. Unfortunately there are not sufficient data for completely filled cylinders to make the necessary crucial comparisons. Most of the experimental data were generated in a gyrostat; the technique of determining C_R and C_I is discussed in Reference 1. The C_I were not measured directly but were determined from the observed maximum rate of divergence of the gyrostat motion and relationships taken from Wedemeyer's theory; the latter fact indicates a possible logical inconsistency in a comparison of Wedemeyer's theory with the experimental C_I.

Results for two values of Re are compared in Table 4 for k = 3, m = 1, n = 1, and c = 3.148; the data in Case I come from Reference 13; Case II was done specifically for this report. Both Wedemeyer's and our results for C_R agree with the experimental values for both cases to within the estimated uncertainty. The data were not accurate enough to obtain C_I for Case I, Re = 5.2×10^5; but from results for partially-filled cylinders we should expect agreement at this Re. For Case II the theoretical and experimental results for C_I agree, considering the accuracy of the latter. Thus, it is an open question whether our results are in fact superior to Wedemeyer's.

---

13. W. P. D'Amico, Jr., private communication.

Table 4. Comparison of Predicted and Measured Eigenfrequencies for Mode m = 1, k = 3, n = 1 for Basic Flow in Solid-Body Rotation.

	Case I: Re = 5.195×10^5		Case II: Re = 8.977×10^3	
	C_R	C_I	C_R	C_I
Gyrostat Measurements	0.048 ± .002	(Insufficient Accuracy)	0.051 ± .003	0.011 ± .002
Stewartson Inviscid Perturbation	0.0462	0	0.0462	0
Wedemeyer Correction to Stewartson Value	0.0468	0.0014	0.0500	0.0104
Result from Present Viscous Perturbation--No Correction	0.0473	0.0009	0.0530	0.0078
Result from Present Viscous Perturbation--Correction δc_s	0.0469	0.0014	0.0505	0.0116

Most of the experiments were conducted with partially-filled cylinders because these are the more practical cases and the filled cylinder experiment is more difficult. Wedemeyer[3] compared his calculations with data obtained from the gyrostat experiments, and the agreement was impressive. The data were obtained for a cylinder of nominally 85% fill-ratio, but the actual value was varied in the experiments. The viscous correction theory of Wedemeyer requires 100% fill-ratio, as does ours. But since he applies his correction to Stewartson's results for partially-filled cylinders, he evidently assumes that it is applicable there also; this assumption seems justified by the favorable comparison. There is no counterpart to Stewartson's results to which our boundary condition correction can be applied; thus a clear-cut check of the two theoretical results against experimental data is not possible. Analysis of the available data and calculations indicates that the difference between the C_I's for 85% and 100% ratios is negligible for $Re \geqslant 10^4$ and $c \cong 3$; however, for $Re \leqslant 10^4$ the effect of fill-ratio on C_I is more pronounced. For example, with $Re = 5.05 \times 10^2$, $c = 3.08$, $k = 3$, $m = 1$, and $n = 1$, Wedemeyer's formulae give $C_I = 0.0490$ (85%) and 0.0437 (100%). Whether or not these accurately represent the effect of fill-ratio at low Re is not known, and appropriate experimental data are not available. Further experimentation is required.

VI. CONCLUSIONS

Although the main objective of the work reported here is to develop methods to compute the eigenvalues for small perturbations of spin-up flow in a cylinder, this Part I is restricted to consideration of solid-body rotation so that the numerical technique can be described in detail without the distraction of the complexities that arise in spin-up, and yet provide results that can be checked with other theoretical work and experimental data. The perturbation equations are solved using an orthonormalization technique to insure linear independence of the solutions, and the eigenvalues are determined iteratively. A correction for the endwall boundary condition is derived and incorporated into the program which then provides eigenvalues that agree with other results in the literature and with experimental data.

ACKNOWLEDGEMENTS

The authors express their appreciation to J. M. Bartos for her assistance in programming and performing the computations. They also wish to acknowledge the help received from W. P. D'Amico, S. Davis, A. Davey, and G. P. Neitzel.

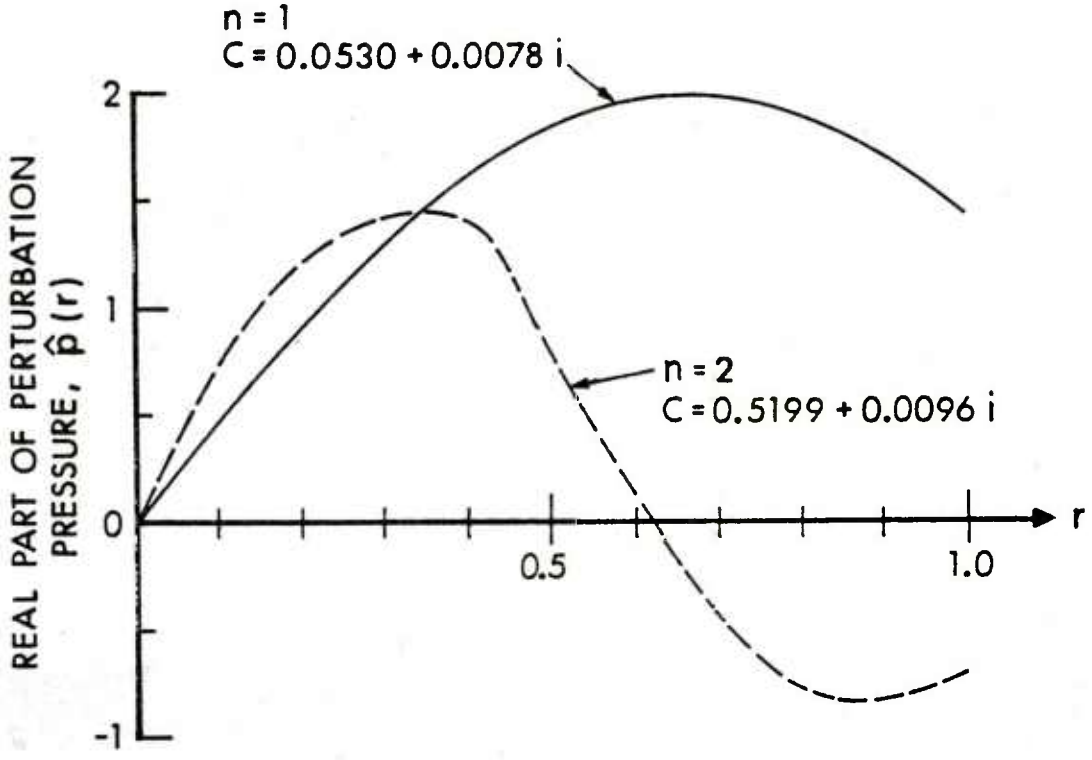

Figure 1. Real part of $\hat{p}(r)$ for two radial modes, with c = 3.15, Re = 8977, m = 1, k = 3.

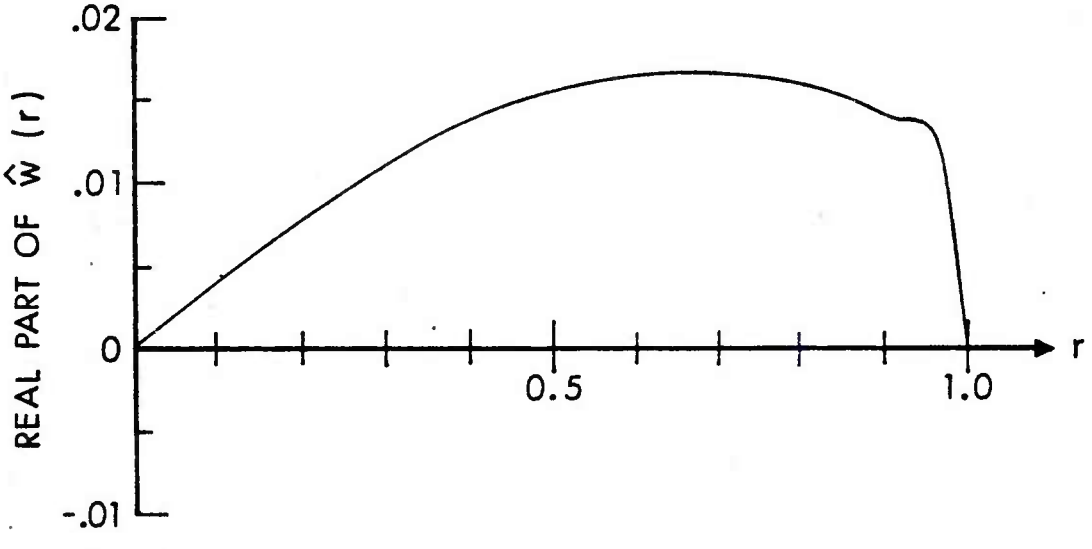

Figure 2. Real part of $\hat{w}(r)$ for n = , with c = 3.15, Re = 8977, m = 1, k = 3.

REFERENCES

1. *Engineering Design Handbook, Liquid-Filled Projectile Design,* AMC Pamphlet No. 706-165, U.S. Army Materiel Development and Readiness Command, Washington, D. C., April 1969. AD 853719.

2. K. Stewartson, "On the Stability of a Spinning Top Containing Liquid," *J. Fluid Mech.*, Vol. 5, Part 4, September 1959, pp. 577-592.

3. E. H. Wedemeyer, "Viscous Corrections to Stewartson's Stability Criterion," BRL Report No. 1325, Aberdeen Proving Ground, Maryland, June 1966. AD 489687.

4. E. H. Wedemeyer, "The Unsteady Flow Within a Spinning Cylinder," *J. Fluid Mech.*, Vol. 20, Part 3, 1964, pp. 383-399. Also, see BRL Report No. 1252, Aberdeen Proving Ground, Maryland, October 1963. AD 431846.

5. Y. M. Lynn, "Free Oscillations of a Liquid During Spin-Up," BRL Report No. 1663, Aberdeen Proving Ground, Maryland, August 1973. AD 769710.

6. R. Sedney and N. Gerber, "Perturbation Equations for Liquid Spin-Up in Cylindrical Cavities," BRL Technical Report (in preparation).

7. S. Godunov, "On the Numerical Solution of Boundary-Value Problems for Systems of Linear Ordinary Differential Equations," *Uspekhi Mat. Nauk.*, Vol. 16, 1961, pp. 171-174.

8. S. D. Conte, "The Numerical Solution of Linear Boundary Value Problems," *SIAM Review,* Vol. 8, 1966, pp. 309-321.

9. M. R. Scott and H. A. Watts, " SUPORT-A Computer Code for Two-Point Boundary-Value Problems via Orthonormalization," Sandia Laboratories Report SAND 75-0198, Albuquerque, New Mexico, June 1975, pp. 89-94.

10. A. Davey, "A Simple Numerical Method for Solving Orr-Sommerfeld Problems," *Quarterly Journal of Mathematics and Applied Mechanics,* Vol. 26, Part 4, 1973, pp. 401-411.

11. E. R. Krueger, A. Gross, and R. C. DiPrima, "On the Relative Importance of Taylor-Vortex and Non-Axisymmetric Modes in Flow Between Rotating Cylinders," *J. Fluid Mech.* (1966), Vol. 24, Part 3, pp. 521-538.

12. P. M. Eagles, "On Stability of Taylor Vortices by Fifth-Order Amplitude Expansions," *J. Fluid Mech.* (1971), Vol. 49, Part 3, pp. 529-550.

REFERENCES (Continued)

13. W. P. D'Amico, Jr., private communication.

LIST OF SYMBOLS

Length, velocity, pressure, and time are non-dimensionalized by a, $a\Omega$, $\rho\Omega^2a^2$, and Ω^{-1}, respectively.

a	cross-sectional radius of cylinder [m]
$\underline{A}^{\lambda}$	3x3 orthogonalization matrix in λth subinterval (see (20))
b	value of r where initial conditions are specified
$\underline{B}^{\lambda}$	3x3 orthonormalization matrix in λth subinterval (see (22))
c	half-height of cylinder
C	$\equiv C_R + iC_I$, complex eigenvalue
C_I	disturbance decay rate/Ω
C_R	disturbance frequency/Ω
D(C)	$\equiv D_R + iD_I$, 3x3 determinant whose zeros are the eigenvalues (see (19))
$\underline{E},\underline{F}$	6x3 matrices specifying initial and terminal conditions, respectively (see (14) and (15))
F	symbol denoting a solution u,v,w,p (Appendix A)
$\underline{G}$	6x6 matrix of coefficients in (9) (see (13))
J	iteration operator -- $C_{\mu+1} = J(C_\mu)$ (see (31))
k,m,n	axial, azimuthal, and radial indices, respectively, of a disturbance mode
K	$= k\pi/(2c)$ (see (7))
N	number of subintervals in orthonormalization
p	pressure
$\overset{*}{p}$	pressure perturbation (see (1))
$\hat{p}$	radial part of pressure perturbation (see (6))

LIST OF SYMBOLS (Continued)

P	unperturbed pressure
r	radial coordinate
Re	$\equiv \Omega a^2/\nu$, Reynolds number
$s_{j1}, \ldots, s_{j6}$	elements of solution vector $\underline{S}_j$
$\underline{S}_j$	eigenvalue problem solution vector, j = 1, 2, 3 (see (16))
$\underline{S}$	3x6 solution matrix whose rows are $\underline{S}_j$ (see (16))
$\underline{\bar{S}}^{\lambda}$	orthogonalized solution matrix in λth subinterval (see (20))
t	time [non-dimensional]
t_{ji}^{λ}	elements of 3x6 matrix $\underline{T}^{\lambda}$
$\underline{T}^{\lambda}$	orthonormalized solution matrix in λth subinterval (see (22))
u,v,w	radial, azimuthal, and axial components, respectively, of velocity
$\overset{*}{u},\overset{*}{v},\overset{*}{w}$	radial, azimuthal, and axial components, respectively, of perturbation velocity (see (1))
$\hat{u},\hat{v},\hat{w}$	radial parts of $\overset{*}{u}$, $\overset{*}{v}$, and $\overset{*}{w}$, respectively (see (6))
U, V, W	radial, azimuthal, and axial components, respectively, of unperturbed velocity
y	boundary layer normal coordinate at endwall (see A.3a-d)
$y_1, \ldots, y_6$	dependent variables in canonical form of eigenvalue differential equation system (see (8))
$\underline{Y}$	solution vector $\{y_1, \ldots, y_6\}$

z	axial coordinate (= 0 at base of cylinder)
α_{ij}^{λ}	elements of $\underline{A}^{\lambda}$ (see (21))
β_{ij}^{λ}	elements of $\underline{B}^{\lambda}$ (see (23))
γ_1, γ_2, γ_3	constant coefficients in (16)
δc_s, δc_w	cylinder half-height correction due to endwall boundary layer--present theory, Wedemeyer theory, respectively
Δ	displacement thickness of endwall boundary layer (see A.6)
$\underline{\Gamma}$	1x3 matrix $\{\gamma_1, \gamma_2, \gamma_3\}$
ϵ	value of r where numerical integration is initiated
θ	azimuthal angle [radians]
ν	kinematic viscosity of fluid [m^2/s]
ρ	density of fluid [kg/m^3]
Ω	spin rate of cylinder [radians/s]

Superscript

λ	subinterval index
$\sim$	endwall boundary layer approximation
$'$	d/dr in (8) and (9)

Subscript

I	imaginary part of complex number
R	real part of complex number
λ	subinterval index

μ	iteration index in solution of $D(C) = 0$ (see (28))
o	solution which satisfies inviscid boundary conditions at endwalls (Appendix A)
1	correction to o solution (Appendix A)
∞	endwall value of o solution

Miscellaneous

$\cdot$	inner product -- $\underline{S}_1 \cdot \underline{S}_2 = \sum_{i=1}^{6} s_{1i}\, s_{2i}$
$\|\|\ \ \|\|$	norm of a vector -- $\|\| \underline{S} \|\|^2 = \underline{S} \cdot \underline{S}$

APPENDIX A: CORRECTION FOR THE ENDWALL BOUNDARY CONDITIONS

The derivation of the correction for endwall boundary conditions, discussed in Section IV, is presented here; this correction is needed to satisfy $\overset{*}{u} = \overset{*}{v} = 0$ on $z = 0, 2c$. The perturbation equations for solid body rotation are (3), the linearized Navier-Stokes equations:

$$(\overset{*}{ru})_r + \overset{*}{v}_\theta + r\overset{*}{w}_z = 0 \tag{A.1a}$$

$$\overset{*}{u}_t + \overset{*}{u}_\theta - 2\overset{*}{v} = -\overset{*}{p}_r + Re^{-1}\,(\nabla^2\,\overset{*}{u} - r^{-2}\,\overset{*}{u} - 2r^{-2}\,\overset{*}{v}_\theta) \tag{A.1b}$$

$$\overset{*}{v}_t + \overset{*}{v}_\theta + 2\overset{*}{u} = -r^{-1}\,\overset{*}{p}_\theta + Re^{-1}\,(\nabla^2\,\overset{*}{v} - r^{-2}\,\overset{*}{v} + 2\,r^{-2}\,\overset{*}{u}_\theta) \tag{A.1c}$$

$$\overset{*}{w}_t + \overset{*}{w}_\theta = -\overset{*}{p}_z + Re^{-1}\,\nabla^2\,\overset{*}{w} \tag{A.1d}$$

where

$$\nabla^2 \equiv \partial^2/\partial r^2 + r^{-1}\,\partial/\partial r + r^{-2}\,\partial^2/\partial\theta^2 + \partial^2/\partial z^2 \quad , \qquad Re = \Omega a^2/\nu \quad .$$

The boundary conditions are $\overset{*}{u} = \overset{*}{v} = \overset{*}{w} = 0$ at $z = 0, 2c$ and at $r = a$. The solution to the problem is denoted by $F \equiv (\overset{*}{u}, \overset{*}{v}, \overset{*}{w}, \overset{*}{p})$.

As discussed in Section II we solve the same equations

$$u_{o_t} + u_{o_\theta} - 2v_o = -p_{o_r} + Re^{-1}\,(\nabla^2\,u_o - r^{-2}\,u_o - 2r^{-2}\,v_{o_\theta}) \tag{A.2a}$$

$$v_{o_t} + v_{o_\theta} + 2u_o = -r^{-1}\,p_{o_\theta} + Re^{-1}\,(\nabla^2\,v_o - r^{-2}v_o + 2\,r^{-2}\,u_{o_\theta}) \tag{A.2b}$$

$$w_{o_t} + w_{o_\theta} = -p_{o_z} + Re^{-1}\,\nabla^2\,w_o \tag{A.2c}$$

$$(r\,u_o)_r + v_{o_\theta} + r\,w_{o_z} = 0 \quad , \tag{A.2d}$$

but with boundary conditions $u_o = v_o = w_o = 0$ at $r = a$, and $w_o = 0$ at $z = 0, 2c$, but $u_o \neq 0$ and $v_o \neq 0$ there. Let F_o denote the solution to this problem, for which a modal analysis in the z direction is possible. Since erroneous values for C_I were obtained with these incorrect

(inviscid) boundary conditions and a modal analysis for F could not be made, a correction to F_o was sought which satisfies the no-slip boundary conditions at z = 0,2c.

Subscript 1 is used to denote the correction. Since F and F_o differ only in their boundary conditions at z = 0,2c, we expect $F - F_o$ to differ from zero only near the end-walls. The correction F_1 should have the property that $u_1 + u_o = v_1 + v_o = w_1 + w_o = 0$ at z = 0,2c, and $F_1 \to 0$ or $F_1 + F_o \to F$, away from this boundary. Thus, $F_1 = F - F_o$ must have a boundary layer character near z = 0,2c; and, because of the similarity of this problem to Wedemeyer's, the same $Re^{-\frac{1}{2}}$ scaling is appropriate to this boundary layer. The boundary layer approximation to F_1 is denoted by $\tilde{F}_1$ and is an approximation to the desired correction, but only in the boundary layer; elsewhere the correction is negligible.

Under the boundary layer approximation $F_1 = F - F_o$ becomes $\tilde{F}_1 = \tilde{F} - \tilde{F}_o$ where $\tilde{F}_o$ is the boundary layer approximation to the solution of (A.2a-d); the $\tilde{F}$, obtained from this relation, is the corrected F_o or the desired F, to within the boundary layer approximation. Let δ_1 be a measure of the thickness of the boundary layer so that $\delta_1 = 0\ (Re^{-\frac{1}{2}})$. Using the form of the solution for F_o in (6a-d) it can be easily shown that $\tilde{F}_o$ satisfies the inviscid equations; i.e., (A.2a-d) with $\nu = 0$, with an error of $0(Re^{-1})$ except near r = a, where the sidewall boundary layer induces a viscous contribution. Also, the changes in u_o and v_o across δ_1 are

$$\Delta u_o = 0\ (Re^{-1}) \quad , \qquad \Delta v_o = 0\ (Re^{-1}) \quad .$$

Thus,

$$\tilde{u} = \tilde{u}_o + \tilde{u}_1 = u_{o\infty} + \tilde{u}_1 \quad , \qquad \tilde{v} = \tilde{v}_o + \tilde{v}_1 = v_{o\infty} + \tilde{v}_1 \quad ,$$

with the same error $0\ (Re^{-1})$, where sub ∞ denotes evaluation on the end-walls z = 0,2c. The conclusions of this paragraph are needed when the displacement surface is determined.

The boundary layer approximation applied to the equations for $F_1 = F - F_o$, yields

$$\tilde{u}_{1_t} + \tilde{u}_{1_\theta} - 2\tilde{v}_1 + \tilde{p}_{1_r} = Re^{-1}\,\tilde{u}_{1_{yy}} \tag{A.3a}$$

$$\tilde{v}_{1_t} + \tilde{v}_{1_\theta} + 2\tilde{u}_1 + r^{-1}\,\tilde{p}_{1_\theta} = Re^{-1}\,\tilde{v}_{1_{yy}} \tag{A.3b}$$

$$\tilde{p}_{1_y} = 0 \tag{A.3c}$$

$$(r\tilde{u}_1)_r + \tilde{v}_{1_\theta} - (r\tilde{w}_1)_y = 0 \tag{A.3d}$$

for the endwall at z = 2c, where y = 2c - z is the boundary layer normal coordinate. The boundary conditions are

$$\left.\begin{aligned} \tilde{u}_1 &= -u_{o\infty} \\ \tilde{v}_1 &= -v_{o\infty} \\ \tilde{w}_1 &= 0 \end{aligned}\right\} \quad \text{at } y = 0\,, \qquad \tilde{u}_1 = \tilde{v}_1 = 0 \text{ at } y = \infty\,.$$

Since the flow F_1 is generated by changing from the no-slip to the inviscid type boundary conditions there is no mechanism to cause pressure gradients. Thus, $p_1 = 0$ and $\tilde{p}_1 = 0$. Then (A.3a-b) are in the same form as Wedemeyer's (28a-b), but their meaning is different. These equations are decoupled by introducing

$$A = \tilde{v}_1 + i\tilde{u}_1\,, \qquad B = \tilde{v}_1 - i\tilde{u}_1\,,$$

and solved assuming the same periodicity, $e^{i(Ct-\theta)}$, as for F_o; i.e., m=1. The results for $\tilde{u}_1$ and $\tilde{v}_1$ are

$$\tilde{u}_1 = (i/2)\,[(v_{o_\infty} + iu_{o_\infty})\,e^{-\alpha y} - (v_{o_\infty} - iu_{o_\infty})\,e^{-\beta y}] \tag{A.4a}$$

$$\tilde{v}_1 = -(1/2)\,[(v_{o_\infty} + iu_{o_\infty})\,e^{-\alpha y} + (v_{o_\infty} - iu_{o_\infty})\,e^{-\beta y}] \tag{A.4b}$$

where

$$\alpha = - Re^{\frac{1}{2}} [(3 - C_R)^2 + C_I^2]^{\frac{1}{4}} e^{i\sigma_1}$$

$$\sigma_1 = (1/2) [\{2 - H (C_I)\} \pi + \tan^{-1} \{(3 - C_R)/C_I\}]$$

$$\beta = - Re^{\frac{1}{2}} [(1 + C_R)^2 + C_I^2]^{\frac{1}{4}} e^{i\sigma_2} \qquad (A.5)$$

$$\sigma_2 = (1/2) [\{2 + H (C_I)\} \pi - \tan^{-1} \{(1 + C_R)/C_I\}]$$

$$H (C_I) = 0 \text{ for } C_I < 0, \quad = 1 \text{ for } C_I > 0.$$

The principal values for $\tan^{-1}$ are used.

Next the displacement surface, $y = \Delta(r, \theta, t)$, is found. This is an impermeable surface in the o flow; i.e., $\tilde{w}_o = 0$ on it. Δ satisfies a first order partial differential equation. as for a steady 3-D boundary layer. For unsteady incompressible flow an additional term, $r\Delta_t$, appears. The equation for Δ is

$$[r\, u_{o\infty} (\Delta - \delta^r)]_r + (v_{o\infty} (\Delta - \delta^\theta)]_\theta + r \Delta_t = 0 \qquad (A.6)$$

where

$$u_{o\infty}\, \delta^r \equiv \int_0^\infty (u_{o\infty} - \tilde{u})\, dy = - \int_0^\infty \tilde{u}_1\, dy$$

$$= (1/2)(\alpha^{-1} + \beta^{-1})\, u_{o\infty} - (i/2)(\alpha^{-1} - \beta^{-1})\, v_{o\infty} \quad ,$$

$$v_{o\infty}\, \delta^\theta \equiv \int_0^\infty (v_{o\infty} - \tilde{v})\, dy = - \int_0^\infty \tilde{v}_1\, dy$$

$$= (1/2)(\alpha^{-1} + \beta^{-1})\, v_{o\infty} + (i/2)(\alpha^{-1} - \beta^{-1})\, u_{o\infty}$$

using (A.4a-b).

After some analysis, employing the order of magnitude estimates for Δu_o and Δv_o given in the paragraph preceding (A.3a-d), (A.6) can be written as

$$[ru_{o\infty}\ (\Delta - \delta)]_r + [v_{o\infty}\ (\Delta - \delta)]_\theta + r\Delta_t = 0 \qquad (A.7)$$

where

$$2\delta = \alpha^{-1} + \beta^{-1} - 2\ (\alpha^{-1} - \beta^{-1})/(1 - C)\ . \qquad (A.8)$$

The only periodic non-singular solution of (A.7) is the constant

$$\Delta = \delta\ .$$

From (A.5), Δ depends only on Re and c, and is easily found after the eigenvalue $C = C_R + iC_I$ is determined for the problem o. Putting $C_I = 0$ in (A.5) and (A.8) gives $\delta = \delta c$ = Wedemeyer's displacement thickness (non-dimensionalized). Wedemeyer also determines a displacement thickness for the sidewall boundary layer. In our problem this is not necessary since the proper boundary conditions are satisfied at the sidewall.

The displacement thickness is a complex constant. The interpretation of the complex Δ is given in Reference 1. Operationally it is used in the same manner as a real displacement thickness: 2c is replaced by $2c - 2\Delta$ and the o problem is re-solved.

APPENDIX B: POWER SERIES COEFFICIENTS

In accordance with Section III.B, analytical solutions to (9) are found for the interval $0 \leq r \leq \varepsilon$. These are obtained by substituting power series for $\hat{u}$, $\hat{v}$, $\hat{w}$, and $\hat{p}$ into (9) and determining the coefficients.

The solution for the azimuthal mode m = 1 is given by

$$\hat{u} = \sum_{j=0} a_j r^j \quad , \qquad \hat{v} = \sum_{j=0} b_j r^j$$

$$\hat{w} = \sum_{j=0} d_j r^j \quad , \qquad \hat{p} = \sum_{j=0} e_j r^j \quad .$$

The coefficients are given by the following sequence of formulas, where b_o, d_1, and e_1 are arbitrary complex constants:

$$a_o = i\, b_o \quad , \qquad b_o = b_o \quad , \qquad d_o = 0 \quad , \qquad e_o = 0$$

$$a_1 = 0 \quad , \qquad b_1 = 0 \quad , \qquad d_1 = d_1 \quad , \qquad e_1 = e_1$$

$$H \equiv Re^{-1} K^2 + i\, C$$

$$a_2 = -(1/4)\, K\, d_1 + (1/8)\, Re\, [b_o\, (iH - 1) + e_1]$$

$$b_2 = -i\,(1/4)\, K\, d_1 - (3i/8)\, Re\, [b_o\, (iH - 1) + e_1] \quad .$$

For $j = 0, 1, 2, \ldots$

$$N_{1j} = Re\, [H\, a_{j+1} - (2\, b_{j+1} + i a_{j+1})]$$

$$N_{2j} = Re\, [H\, b_{j+1} + (2\, a_{j+1} - i b_{j+1})]$$

$$N_j = [N_{1j} - i\,(j + 2)\, N_{2j}]/[(j + 1)(j + 3)]$$

$$d_{j+2} = Re\ [(H - i)\ d_j - K\ e_j]/[(j + 1)(j + 3)]$$

$$a_{j+3} = -\ [N_j + (j + 4)\ K\ d_{j+2}]/[(j + 5)(j + 3)]$$

$$b_{j+3} = i\ [K\ d_{j+2} + (j + 4)\ N_j]/[(j + 5)(j + 3)]$$

$$e_{j+2} = [2\ a_{j+3} + i\ (j^2 + 6j + 7)\ b_{j+3} - i\ N_{2j}]/Re\ .$$

DISTRIBUTION LIST

No. of Copies	Organization
12	Commander Defense Documentation Center ATTN: DDC-TCA Cameron Station Alexandria, VA 22314
1	Commander US Army Materiel Development and Readiness Command ATTN: DRCDMD-ST 5001 Eisenhower Avenue Alexandria, VA 22333
1	Commander US Army Aviation Research and Development Command ATTN: DRSAV-E 12th and Spruce Streets St. Louis, MO 63166
2	Commander US Army Air Mobility Research and Development Laboratory ATTN: SAVDL-D, W.J.McCroskey Ames Research Center Moffett Field, CA 94035
1	Commander US Army Electronics R&D Command Technical Support Activity ATTN: DELSD-L Fort Monmouth, NJ 07703
1	Commander US Army Communications Rsch and Development Command ATTN: DRDCO-SGS Fort Monmouth, NJ 07703
1	Commander US Army Jefferson Proving Ground ATTN: STEJP-TD-D Madison, IN 47250
2	Commander US Army Missile Research and Development Command ATTN: DRDMI-R DRDMI-TD, Mr. R. Deep Redstone Arsenal, AL 35809
1	Commander US Army Missile Materiel Readiness Command ATTN: DRSMI-AOM Redstone Arsenal, AL 35809
1	Commander US Army Tank Automotive Research & Development Cmd ATTN: DRDTA-UL Warren, MI 48090
1	Commander US Army Armament Materiel Readiness Command ATTN: DRSAR-LEP-L, Tech Lib Rock Island, IL 61299
3	Commander US Army Armament Research and Development Command ATTN: DRDAR-LCA-F, A. Loeb DRDAR-TSS (2 cys) Dover, NJ 07801
1	Director US Army TRADOC Systems Analysis Activity ATTN: ATAA-SL, Tech Lib White Sands Missile Range NM 88002

DISTRIBUTION LIST

No. of Copies	Organization
1	Commander US Army Research Office ATTN: Dr. R. E. Singleton P.O. Box 12211 Research Triangle Park North Carolina 27709
1	Commander US Army Waterways Experiment Station ATTN: R. H. Malter Vicksburg, MS 39180
1	AGARD-NATO ATTN: R. H. Korkegi APO New York 09777
3	Commander US Naval Air Systems Command ATTN: AIR-604 Washington, DC 20360
3	Commander US Naval Ordnance Systems Command ATTN: ORD-0632 ORD-035 ORD-5524 Washington, DC 20360
2	Commander David W. Taylor Naval Ship Research and Development Command ATTN: H. J. Lugt, Code 1802 S. de los Santos Head, High Speed Aero Division Bethesda, Maryland 20084
1	Commander US Naval Surface Weapons Center ATTN: DX-21, Lib Br. Dahlgren, Virginia 22448
6	Commander US Naval Surface Weapons Center Applied Aerodynamics Division ATTN: K. R. Enkenhus M. Ciment K. Lobb S. M. Hastings A. E. Winklemann W. C. Ragsdale Silver Spring, MD 20910
1	AFATL (DLDL, Dr. D. C. Daniel) Eglin AFB, Florida 32542
2	AFFDL (W. L. Hankey; J. S. Shang) Wright-Patterson AFB Ohio 45433
6	Director National Aeronautics and Space Administration ATTN: D. R. Chapman J. Marvin J. D. Murphy J. Rakich W. C. Rose B. Wick Ames Research Center Moffett Field, CA 94035
5	Director National Aeronautics and Space Administration ATTN: J. E. Carter E. Price J. South J. R. Sterrett Tech Library Langley Research Center Langley Station Hampton, Virginia 23365

DISTRIBUTION LIST

No. of Copies	Organization
1	Director National Aeronautics and Space Administration Lewis Research Center ATTN: MS 60-3, Tech Lib 21000 Brookpark Road Cleveland, Ohio 44135
2	Director National Aeronautics and Space Administration Marshall Space Flight Center ATTN: A. R. Felix, Chief S&E-AERO-AE Dr. W. W. Fowlis Huntsville, AL 35812
2	Director Jet Propulsion Laboratory ATTN: L. M. Mark Tech Library 4800 Oak Grove Drive Pasadena, CA 91103
3	ARO, Inc. ATTN: J. D. Whitfield R. K. Matthews J. C. Adams Arnold AFB, TN 37389
3	Aerospace Corporation ATTN: T. D. Taylor H. Mirels R. L. Varwig Aerophysics Lab. P.O. Box 92957 Los Angeles, CA 90009
1	AVCO Systems Division ATTN: B. Reeves 201 Lowell Street Wilmington, MA 01887
3	The Boeing Company Commercial Airplane Group ATTN: W. A. Bissell, Jr. M. S. 1W-82, Org 6-8340 P. E. Rubbert J. D. McLean Seattle, WA 98124
2	Calspan Corporation ATTN: A. Ritter M. S. Holden P.O. Box 235 Buffalo, New York 14221
1	Center for Interdisciplinary Programs ATTN: Victor Zakkay W. 177th Street & Harlem River Bronx, New York 10453
1	General Dynamics ATTN: Research Lib 2246 P. O. Box 748 Fort Worth, Texas 76101
1	General Electric Company ATTN: H. T. Nagamatsu Research and Development Laboratory (Comb. Bldg.) Schenectady, New York 12301
1	General Electric Company, RESD ATTN: R. A. Larmour 3198 Chestnut Street Philadelphia, PA 19101
3	Grumman Aerospace Corporation ATTN: R. E. Melnik L. G. Kaufman B. Grossman Research Department Bethpage, New York 11714

DISTRIBUTION LIST

No. of Copies	Organization
2	Lockheed-Georgia Company ATTN: B. H. Little, Jr. G. A. Pounds Dept. 72074, Zone 403 86 South Cobb Drive Marietta, Georgia 30062
1	Lockheed Missiles and Space Company ATTN: Tech Info Center 3251 Hanover Street Palo Alto, California 94304
4	Martin-Marietta Laboratories ATTN: S. H. Maslen S. C. Traugott K. C. Wang H. Obremski 1450 S. Rolling Road Baltimore, Maryland 21227
2	McDonnell Douglas Astronautics Corporation ATTN: J. Xerikos H. Tang 5301 Bolsa Avenue Huntington Beach, CA 92647
1	McDonnell-Douglas Corporation Douglas Aircraft Company ATTN: T. Cebeci 3855 Lakewood Boulevard Long Beach, California 90801
1	Northrup Corporation Aircraft Division ATTN: S. Powers 3901 W. Broadway Hawthorne, California 90250
2	Sandia Laboratories ATTN: F. G. Blottner Tech Lab Albuquerque, NM 87115
2	United Aircraft Corporation Research Laboratories ATTN: R. W. Briley Library East Hartford, CT 06108
1	Vought Systems Division LTV Aerospace Corporation ATTN: J. M. Cooksey Chief, Gas Dynamics Lab., 2-53700 P. O. Box 5907 Dallas, Texas 75222
3	California Institute of Technology ATTN: Tech Library H. B. Keller Mathematics Dept. D. Coles Aeronautics Dept. Pasadena, California 91109
1	Cornell University Graduate School of Aero Engr ATTN: Library Ithaca, New York 14850
2	Illinois Institute of Technology ATTN: M. V. Morkovin H. M. Nagib 3300 South Federal Chicago, Illinois 60616

DISTRIBUTION LIST

No. of Copies	Organization
2	The Johns Hopkins University ATTN: S. H. Davis S. Corrsin Dept. of Mechanics and Materials Science Baltimore, Maryland 21218
1	Louisiana State University Department of Physics ATTN: R. G. Hussey Baton Rouge, LA 70803
3	Massachusetts Institute of Technology ATTN: E. Covert H. Greenspan Tech Library 77 Massachusetts Avenue Cambridge, MA 02139
2	North Carolina State University Mechanical and Aerospace Engineering Department ATTN: F. F. DeJarnette J. C. Williams Raleigh, NC 27607
1	Notre Dame University ATTN: T. J. Mueller Dept. of Aero Engr South Bend, Indiana 46556
2	Ohio State University Dept. of Aeronautical and Astronautical Engineering ATTN: S. L. Petrie O. R. Burggraf Columbus, Ohio 43210
2	Polytechnic Institute of New York ATTN: G. Moretti S. G. Rubin Route 110 Farmingdale, NY 11735
4	Princeton University James Forrestal Research Center Gas Dynamics Laboratory ATTN: I. E. Vas S. M. Bogdonoff S. I. Cheng Tech Library Princeton, NJ 08540
1	Purdue University Thermal Science & Prop Center ATTN: D. E. Abbott W. Lafayette, IN 47907
1	Rensselaer Polytechnic Institute Department of Math. Sciences ATTN: R. C. DiPrima Troy, NY 12181
1	Rutgers University Department of Mechanical, Industrial and Aerospace Engineering ATTN: R. H. Page New Brunswick, NJ 08903
1	Southern Methodist University Department of Civil and Mechanical Engineering ATTN: R. L. Simpson Dallas, TX 75275
1	Southwest Research Institute Applied Mechanics Reviews 8500 Culebra Road San Antonio, TX 78228
1	University of California-Berkeley Department of Aerospace Engineering ATTN: M. Holt Berkeley, CA 94720

DISTRIBUTION LIST

No. of Copies	Organization
1	University of California-Davis ATTN: H. A. Dwyer Davis, CA 95616
2	University of California-San Diego Department of Aerospace Engineering and Mechanical Engineering Sciences ATTN: P. Libby Tech Library La Jolla, CA 92037
2	University of Cincinnati Department of Aerospace Engineering ATTN: R. T. Davis M. J. Werle Cincinnati, OH 45221
1	University of Colorado Department of Astro-Geophysics ATTN: E. R. Benton Boulder, CO 80302
1	University of Hawaii Department of Ocean Engineering ATTN: G. Venezian Honolulu, HI 96822
2	University of Maryland ATTN: W. Melnik J. D. Anderson College Park, MD 20740
1	University of Michigan Department of Aeronautical Engineering ATTN: Tech Library East Engineering Building Ann Arbor, MI 48104
1	University of Santa Clara Department of Physics ATTN: R. Greeley Santa Clara, CA 95053
3	University of Southern California Department of Aerospace Engineering ATTN: T. Maxworthy P. Weidman L. G. Redekopp Los Angeles, CA 90007
1	University of Texas Department of Aerospace Engineering ATTN: J. C. Westkaemper Austin, TX 78712
1	University of Virginia Department of Aerospace Engineering and Engineering Physics ATTN: I. D. Jacobson Charlottesville, VA 22904
1	University of Washington Department of Mechanical Engineering ATTN: Tech Library Seattle, WA 98195
1	University of Wyoming ATTN: D. L. Boyer University Station Laramie, WY 82071
2	Virginia Polytechnic Institute Department of Aerospace Engineering ATTN: G. R. Inger F. J. Pierce Blacksburg, VA 24061

DISTRIBUTION LIST

No. of Copies	Organization
1	Woods Hole Oceanographic Institute ATTN: J. A. Whitehead Woods Hole, MA 02543

Aberdeen Proving Ground

Dir, USAMSAA

Cdr, USATECOM
ATTN: DRSTE-SG-H

Cdr/Dir, USA CSL, EA
ATTN: Munitions Sys Div
Bldg. 3330
E. A. Jeffers
W. C. Dee
W. J. Pribyl
Armament Concepts Ofc
Bldg. 3516 (DRDAR-ACW)
M. C. Miller